CASE FILE
COPY

NOISE RESPONSE OF CAVITIES
OF VARYING DIMENSIONS
AT SUBSONIC SPEEDS

Patricia J. W. Block

Langley Research Center
Hampton, Va. 23665

NOISE RESPONSE OF CAVITIES OF VARYING DIMENSIONS
AT SUBSONIC SPEEDS

Patricia J. W. Block
Langley Research Center

SUMMARY

An expression including the effect of the length-to-depth ratio is obtained to predict the resonant frequencies of a flow-excited cavity and is shown to be in good agreement with experimental results. Interaction between the lengthwise vortical-acoustic modes and the depthwise standing-wave modes is shown to occur at Mach numbers between 0.1 and 0.5. A simple expression for the Mach number at which maximum-amplitude response occurs is derived on the basis of the interaction, and the onset Mach number is found to be slightly lower. The effect of the cavity dimensions on the type of noise spectra produced by the cavity is investigated. A circular-faced and a square cavity are compared as noise generators in a flow.

INTRODUCTION

In view of possible future reduction in certification levels for overall aircraft noise and of the recent advances in propulsive noise suppression, airframe noise reduction has become an important research objective. This objective has engendered the study of non-propulsive flow-surface interaction noise sources found on the airframe. One such noise source, the flow-excited cavity, can be used to model several structures on the airframe, in particular the landing gear wells.

The literature contains many papers on large-amplitude internal pressure oscillations found inside a flow-excited cavity. A review of this literature may be found in reference 1. There is very little information, however, concerning the sound generated by such an arrangement. It was shown in reference 1, where external or farfield sound measurements of a flow-excited cavity were made, that most but not all of the modes of the internal pressure fluctuations radiate as sound. Analytical models and flow visualizations contained in the work on internal pressure oscillations are helpful, therefore, in assessing the important parameters of noise generation.

The prediction of the lengthwise internal oscillation frequencies reported in reference 2 provides a semiempirical relationship for the Strouhal number, or nondimensional frequency, based on the cavity streamwise length. However, the dependence of Strouhal

number on cavity length-to-depth ratio from this relationship proved to be contrary to the experimental results of the present study. The analysis of reference 3 gives physical significance to the empirical constants in the Strouhal relationship of reference 2; however, no dependence on length-to-depth ratio was obtained in the final result. This paper extends the work of reference 3 to include the effect of length-to-depth ratio on Strouhal number.

Other investigators (refs. 4 and 5) have studied the depthwise modes that occur in cavities whose length-to-depth ratio is less than about 2. In this paper these results are written in the form of a Strouhal number also based on length for purposes of comparison with the Strouhal number of the lengthwise oscillation. On the basis of this comparison, a quantitative explanation is given for the interaction or coupling between lengthwise and depthwise modes observed in reference 1. Also a simple expression for the approximate Mach number at which oscillations begin in a cavity is obtained.

An additional purpose of this paper is to gain insight regarding the important param eters of sound generation by a cavity in a flow. This experimental study includes measur ments of noise produced by cavities (rectangular and circular faced) of varying dimensior in a subsonic flow. Special emphasis was given to the spectral shape of the noise for the purpose of delineating regions of broadband or narrowband source behavior as a function of the flow velocity and cavity shape. Noise measurements were made in a reverberant environment over a Mach number range from 0.1 to 0.5. The cavity length-to-depth ratic varied from 0.3 to 8.0 and the length-to-width ratio varied from 0.3 to 1.85.

SYMBOLS

A,B   constants in equations (5), (6), and (7) having empirical values of 0.65 and 0.7 respectively

a   speed of sound, m/sec

C   proportionality constant

D   cavity depth, cm

f   frequency, kHz

H,h   magnitude and phase, respectively, of summation of monopole sources in equation (B6)

$H_0^{(1)}$ Hankel function of first kind

h_0, h_1 intercept and slope, respectively, of phase function h when plotted against $\omega L/a$ (see eq. (B9))

J_0 Bessel function of first kind

K_v ratio of average vortex convection velocity across cavity mouth to free-stream velocity, taken to be 0.57

k_r, k_i real and imaginary parts of complex wave vector in x-direction

L cavity length (streamwise direction), cm

L_p acoustic pressure level, dB (re 20 μPa)

L_w acoustic power level, dB (re 1 pW)

M free-stream Mach number

m mass of fluid

N_{St} Strouhal number

n mode or stage number of vortical-acoustic oscillation

P acoustic pressure

p rms acoustic pressure

Q ratio of center frequency to bandwidth of response of an oscillator

R_A specific acoustic radiation resistance

r radial distance from acoustic source

S acoustic source strength

t time

U_r radial acoustic velocity

U_∞	free-stream velocity, m/sec
W	cavity width (cross-stream direction), cm
X_A	specific acoustic radiation reactance
x,y	rectangular coordinates
Y_0	Bessel function of second kind
α	empirical constant in equation (2)
β	phase difference between source and shear layer displacement at trailing edge
η	displacement of shear layer in y-direction
ρ	fluid density
ϕ	lag of shear layer displacement behind forcing mechanism at leading edge of cavity
ω	angular frequency, $2\pi f$

Subscripts:

d	depthwise standing-wave oscillation
l	lengthwise vortical-acoustic oscillation

Abbreviations:

ANRL	aircraft noise reduction laboratory
MIC	microphone
rms	root mean square
rpm	revolutions per minute

TEST APPARATUS AND PROCEDURE

This experiment was carried out in two different reverberant environments, each having subsonic flow capability. These facilities were the Langley 55-foot vacuum cylinder and the reverberation room of the Langley aircraft noise reduction laboratory (ANRL).

Langley 55-Foot Vacuum Cylinder

Facility.- The vacuum cylinder is 55 feet in diameter with a hemispherical top (fig. 1(a)) and a volume of 3794 m^3. To obtain flow over the cavity, the cylinder is partially evacuated and the cylinder pressure read. The air is exhausted into the cylinder through a 6.35-cm by 25.4-cm rectangular nozzle (fig. 1(b)) with a pneumatically controlled conical inlet port plug. The velocity of the air through the nozzle was computed according to the compressible flow tables from the difference between the atmospheric pressure and the cylinder pressure which was read continuously. This method provided an absolute velocity within 1 percent of that obtained in previous calibrations using a pitot-static tube; however, during a run the pressure differential, thus the velocity, varied. The variation in velocity during a run amounted to ±5 percent of the average velocity for a Mach number of 0.17 and less than ±2 percent for a Mach number of 0.5.

Test setup.- The nozzle guided the flow parallel to a flat 1.2-m-square plate in which the cavity was located (fig. 1(b)). The cavities used in this facility had a fixed depth of 3.81 cm. The length (streamwise direction) and width were varied independently from 2.54 cm to 7.62 cm. A circular-faced cavity with a diameter of 7.62 cm was also tested. The test conditions for this experiment are given in table I.

Acoustic measurement.- Acoustically, the inside of the cylinder, where sound measurements were made, was highly reverberant with a mean reverberation time of 10 sec. Although this facility was not designed as a reverberation chamber, previous acoustic calibrations (ref. 6) demonstrated the suitability of this facility for acoustic research and also its reverberant characteristics at the measurement position. By using these calibrations, a single one-half-inch condenser-type microphone was placed inside the chamber where the acoustic field was known to be reverberant. All rms pressure levels were converted to acoustic power levels as specified in the American National Standard S1.21-1972 (ref. 7) using the 1-kHz reverberation time. Since the reverberation time changes with frequency, conversion of the data using a single reverberation time (viz, that of 1 kHz) leads to a small error in the power level across the spectrum. A correction for this error has not been applied to the data since comparisons of a qualitative nature only are presented herein. The corrections, however, are provided in appendix A for those interested in obtaining the true power levels across the entire frequency range. The barometric pressure change in the chamber from the highest velocity to the lowest amounted to a

correction to the acoustic power of less than 0.1 dB. This correction was less than the accuracy of the spectral amplitude estimates which were about 1 dB.

The data were obtained on line by means of the microphone with a preamplifier, filter, amplifier, Fourier analyzer, and X-Y plotter. Narrowband spectra from 0 to 5 kHz were obtained from the microphone for each test condition. The frequency resolution was 20 Hz for all spectra.

Langley ANRL Reverberant Chamber

Facility.- The ANRL reverberation room is shown in figure 2(a). The air is provided by a centrifugal compressor through a 30-cm by 60-cm rectangular nozzle. The velocity through the nozzle was calibrated with a pitot-static probe and was controlled by setting the compressor rpm. The error in velocity with this method was less than 4 percent. In this facility, Mach numbers from 0.09 to 0.18 were achieved with this nozzle.

Test setup.- The nozzle directed the flow over a flat plate in which the cavity was situated (fig. 2(b)). This cavity had a fixed streamwise length of 4.05 cm and a width of 7.45 cm. The depth was varied from 0 to 13 cm. The test conditions in this facility are listed in table II.

Acoustic measurement.- The ANRL reverberation room is a rectangular chamber having splayed walls and a mean reverberation time of approximately 8 sec for frequencies above 250 Hz. Three one-half-inch condenser-type microphones were mounted inside the chamber and positioned in the reverberant or diffuse field. This was done by suspending a calibrated broadband source in place of the cavity and positioning the microphones until all were recording the same spectra. Subsequent analysis of the cavity noise data from the three microphones showed agreement within 2 dB across the frequency range for all conditions. Narrowband spectra were obtained from all microphones from 0 to 10 kHz. Only the frequencies of the cavity oscillations are reported in this study. Consequently no spectral amplitude correction need be applied.

Data were recorded on magnetic tape and analyzed by a digital computer. Outputs consisted of narrowband spectra with frequency resolution of 20 Hz.

ANALYSIS

Background

Several investigators (refs. 1, 2, 4, 5, and 8 to 10) have recorded the frequencies of oscillation of flow-excited cavities. The Strouhal number,

$$N_{St} = \frac{fL}{U_\infty} \tag{1}$$

was observed to change slowly with Mach number. Rossiter (ref. 2) obtained the following empirical relationship for $N_{St,l}$ (the Strouhal number for lengthwise oscillations) for $M \gtrsim 0.4$:

$$N_{St,l} = \frac{fL}{U_\infty} = \frac{n - \alpha}{\left(1/K_v\right) + M} \qquad (2)$$

Here, n is the stage or mode number, α is an empirical constant which increases as the length-to-depth ratio L/D increases, K_v is the ratio of the vortex convection velocity across the cavity mouth to the free-stream velocity, and M is the Mach number. The value for α that is generally considered to produce the best fit is 0.25.

Figure 3 shows Strouhal numbers obtained in several investigations plotted against Mach number. The value of L/D at each data point indicated by a test-point symbol is given in the key. The solid curves represent the first three modes of equation (2) where $K_v = 0.57$ and $\alpha = 0.25$. The data for values of $M \leq 0.4$ generally indicate that $N_{St,l}$ increases as L/D increases at a given Mach number. This implies that the Strouhal number is a function of L/D and that the dependence is inverse to that implied by equation (2). These data include cases where the cavity depth was varied and where the streamwise length was varied to achieve the given L/D ratios.

Also of note in figure 3 is the fact that for the Mach number range of interest (viz, $0.1 \leq M \leq 0.4$), the L/D ratio of the cavities is less than about 4.0, although cavities of larger L/D were tested. Therefore, to improve the existing prediction methods for the middle and lower Mach number range, one should include the cavity depth by way of the L/D ratio and also consider other oscillatory phenomena common in cavities whose length-to-depth ratio is less than about 4.0. Other such phenomena include depthwise standing-wave modes and the volume-dependent Helmholtz oscillation.

Another motivation for considering these other oscillatory phenomena stems from observations (ref. 1) that coupling or interaction between the lengthwise, or vortical-acoustic, oscillations and the depthwise modes does occur in some situations. When the frequency of the lengthwise oscillation, which is not purely acoustic but depends on vortex shedding, approaches the frequency of the depthwise standing-wave modes, considerable amplification of the radiated sound occurs. In cavities whose ratio of volume to surface area is large, the Helmholtz oscillation would be considered, but for the rectangular cavities tested herein, it is believed that the depthwise standing-wave oscillation is present.

Resonant Frequency Prediction

Lengthwise oscillations.- Several investigations (see ref. 1 for review) of cavity oscillation have concluded that a feedback mechanism, such as is found in edgetone production, is the cause of the large-amplitude pressure oscillations found inside a flow-

excited shallow rectangular cavity. This idea is pursued here to predict the frequencies of this feedback phenomenon which is found in cavities where streamwise oscillation occurs. The problem is shown in the following sketch and described as follows:
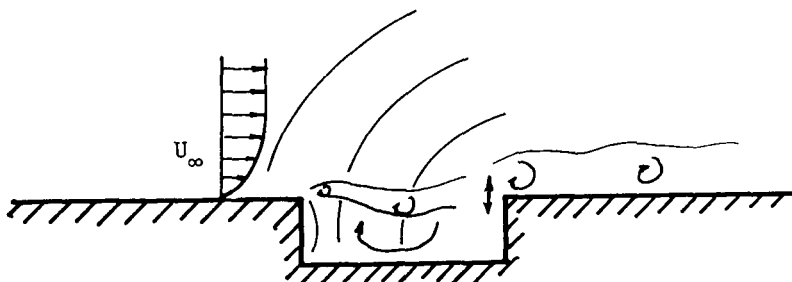
A shear layer between the outer free-stream flow and the secondary cavity flow is formed as the flow passes over the cavity. Flow visualization techniques (ref. 10) have shown three outstanding features of this flow. First, discrete vortices are clearly seen in the shear layer over the cavity and downstream of the cavity trailing edge. Second, acoustic radiation is observed originating at the trailing edge. Third, the secondary flow observed in the cavity and the shedding of vortices at the trailing edge are related to the up-and-down motion of the shear layer at the trailing edge.

The feedback path is constructed as follows. The action of the shear layer on the trailing edge generates sound which travels upstream to the leading edge of the cavity. Here the unstable shear layer responds to the difference in pressure between the acoustic wave above the cavity which continues to travel upstream, and the acoustic wave below the shear layer which is reflected from the front wall of the cavity. This response causes th shear layer to roll up and form a vortex which travels downstream, interacts with the trailing edge to produce sound, and begins the feedback loop again.

For analysis purposes the cavity is modeled in two dimensions as seen in the follov ing sketch. The shear layer is modeled by an infinitely thin sheet along which the distur- bance or vortex travels and whose motion may be described as a growing sinusoid. The
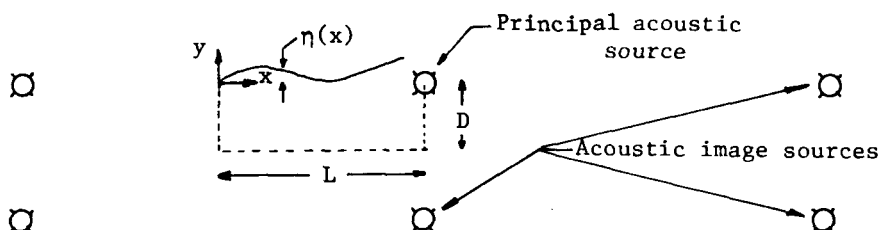
acoustic source at the trailing edge is represented as a simple source. To meet the boundary conditions on the internal cavity walls, image sources are used; however, thes

do not satisfy the boundary conditions on the plate in which the cavity is located. The acoustic field and the motion of the shear layer, which are the two elements involved in this feedback loop, are matched at the points $x = 0, y = 0$ and $x = L, y = 0$. The analysis of this feedback mechanism, which is provided in appendix B, leads to the following relationship for the Strouhal number (eq. (B12)) which is dependent on length-to-depth ratio:

$$N_{St,l} = \frac{fL}{U_\infty} = \frac{n}{\frac{1}{k_r} + M\left(1 + \frac{0.514}{L/D}\right)} \tag{3}$$

where k_r is the real part of the wave number of the disturbance traveling downstream and n is the mode number. This is one of the principal theoretical findings of this study. Equation (3) differs from equation (2) in the variation of $N_{St,l}$ with L/D.

Depthwise modes.- In reference 4 the following expression was obtained to describe the pressure amplitude as a function of frequency over the mouth of the cavity for the depthwise modes:

$$p \propto \left[\left(R_A \sin \frac{2\pi fD}{a} \right)^2 + \left(X_A \sin \frac{2\pi fD}{a} - \cos \frac{2\pi fD}{a} \right)^2 \right]^{-1/2} \tag{4}$$

where R_A and X_A represent the real and imaginary parts of the acoustic impedance of the cavity mouth. They depend on the cavity length and width, the Mach number, and the frequency. The frequencies of depthwise oscillations occur at the maxima of equation (4) with the first maximum being the first depthwise mode and the only one of interest. The lowest (frequency) depthwise mode for each of the cavities tested herein has been obtained from equation (4); however, this is an involved calculation to perform. (See ref. 4.)

An alternative approach is offered in reference 5 where the locus of the maxima of equation (4) as a function of depth is obtained for the particular cavity used in that study by

$$\frac{fD}{a}\left[1 + A\left(\frac{L}{D}\right)^B \right] = \frac{1}{4} \tag{5}$$

The constants A and B have the empirical values of 0.65 and 0.75, respectively. The comparison between equation (5) and the locus of maxima of equation (4) as a function of depth for the cavities used in this study is seen in a subsequent section.

Equation (5) may be rewritten in a form more convenient for present purposes as

$$N_{St,d} = \frac{fL}{U_\infty} = \frac{1}{M}\frac{L}{D}\frac{1/4}{1 + A\left(\frac{L}{D}\right)^B} \tag{6}$$

This Strouhal number is based on length so that comparison with equation (3) may be made on the same nondimensional basis. Equation (6) also provides an expression that is dependent on L/D and that varies inversely with the Mach number.

Maximum-amplitude and onset Mach number.- Equations (3) and (6) predict the frequency (nondimensionalized by the same variables) of cavity oscillation in the lengthwise and depthwise modes, respectively. Reinforcement of one type of oscillation by the other should occur at the Mach number where these frequencies coincide. Therefore, equations (3) and (6) are equated and the resulting expression is solved for Mach number to obtain

$$M = \frac{\frac{1}{k_r}\frac{L}{D}}{4n\left[1 + A\left(\frac{L}{D}\right)^B\right] - \left(\frac{L}{D} + 0.514\right)} \tag{7}$$

This simple equation predicts the Mach number at which maximum-amplitude response occurs in a cavity of given L/D in a given mode. The onset Mach number occurs at a lower value than that predicted by equation (7). The data presented in the next section indicate that the onset Mach number may be as much as 10 percent lower. It is believed that this equation is appropriate for cavities with L/D ratios up to 2 and in the Mach number range from 0.1 to 0.5.

RESULTS AND DISCUSSION

Strouhal Relationships

The data for this study are divided into two groups: those taken in the Langley 55-foot vacuum cylinder where Mach numbers up to 0.5 were attained and those taken in the Langley ANRL reverberation room where $M < 0.2$. These data along with equations (3) and (6) are plotted in figure 4. The solid and short-dashed curves are a plot of Strouhal number as a function of Mach number for the depthwise standing-wave oscillation for three values of L/D. These vary as $1/M$. The short-dashed curves are computed from equation (6). The solid curves are the loci of maxima of equation (4) using the dimensions of the particular cavities used in this study.

The long-dashed curves represent Strouhal number for three modes of the length-wise, or vortical-acoustic, feedback oscillations computed from equation (3). These curves vary slowly with M. Again, for each mode, the curves have been plotted for three values of L/D.

The experimental data consist of the frequency of cavity oscillation normalized by the cavity length and flow velocity, to form the Strouhal number (eq. (1)), plotted against Mach number. The L/D value of the cavity from which each data point was taken is indicated by the test-point symbol in the key.

Effect of length-to-depth ratio.- As is seen in both equations (3) and (6) and graphically in figure 4, the predicted Strouhal number increases at a given Mach number as L/D increases. The data from each experiment show this same trend. In figure 4(a) the length was varied to give a certain L/D; in figure 4(b) the depth was varied. In each case the Strouhal number of the data increased with increasing L/D at a given Mach number.

Further, note in figure 4 that the ability of equation (6) to predict the frequencies of the depthwise standing-wave oscillation (locus of maxima of eq. (4)) diminishes as L/D increases.

Interaction of lengthwise and depthwise modes.- In figure 4(a) the data lie near a curve corresponding to either type of oscillation, generally in the vicinity of the intersection of the two types of curves. The data for smaller values of L/D (deeper cavities) tend to follow the depthwise standing-wave oscillation curves as would be expected. This occurs at the lower Mach numbers around M = 0.1 where the slope of the standing-wave curves is very steep. (The steep slope could produce the scattered effect which was seen in fig. 3.) The data do not tend to follow these standing-wave curves continuously (see also fig. 4(b)) but rather the data are clustered in the vicinity of the intersection with the curves of lengthwise vortical-acoustic oscillation (short-dashed curves).

This interaction also occurs for the shallower cavities as in the case where the L/D = 2 (fig. 4(a)). The data follow the lines of vortical-acoustic oscillation, but appear to begin in the vicinity of the intersection with the lines of standing-wave oscillation. (This interaction of the two types of oscillation results in the self-limiting effect mentioned in appendix B which gave a basis for the use of a straight line to approximate the phase in eq. (B9), even for small values of L/D.) Recall that the intersection of the two types of curves corresponds to the Mach number at which maximum-amplitude response occurs. The data (fig. 4(a)) indicate that the onset Mach number is slightly lower.

A similar pattern is found in figure 4(b). Note, for example, that for L/D = 0.81 to 1.35, no oscillations were recorded in mode 1. This results because the curves of standing-wave oscillation intersect the mode 1 vortical-acoustical curves at a Mach number which is greater than the highest velocity attained during the test. Also,

cavities with L/D ratios of 2, 4, and 8 were tested in the ANRL reverberation room and did not oscillate at all. Figure 4(b) indicates that for L/D of 2 and greater, the curves of standing-wave oscillation would intersect the lengthwise oscillation curves at a Mach number greater than 0.175. This was the highest Mach number attainable in ANRL with the particular test setup, yet it was too low to permit oscillation at these values of L/D in any of the first three modes. The range of Mach numbers over which this interaction occurs for a given cavity is a function of Q or the width of the cavity and is discussed subsequently.

Change in Noise Spectra With Velocity

Spectral features of several of the cavity modes and their development with velocity may be seen in figure 5. The 16 frames show the measured noise power spectrum in dB from 0 to 3 kHz produced by the cavity at the velocities listed. The cavity for this sequence was 2.54 cm long, 7.62 cm wide, and 3.81 cm deep. (The amplitude correction for this frequency range from appendix A is less than 3 dB and does not appreciably change the shape of the spectra.) The velocity is decreasing from the upper left frame (M ≈ 0.5) to the lower right frame (M ≈ 0.1). All spectra are to the same scale, which is indicated in the last frame, and have been set one above the other with individual scales eliminated to facilitate comparison.

In the first frame where the velocity is 168 m/sec, the spectrum shows no tone and, in fact, coincides with the background noise spectrum for this velocity; that is, the cavity is transparent to the flow. In this case the shear layer above the cavity spans the length of the cavity without turning in and out. This turning in and out maintains the feedback mechanism discussed previously. This phenomenon where the cavity is transparent to the oscillation mechanism has been observed by Karamcheti (ref. 10) who also noted that the minimum cavity length required for oscillation was a function of velocity.

Subsequent frames show the development of an intense tone which increases and then decreases in amplitude as the velocity decreases from 147 m/sec to 61 m/sec. The frequency of the tone decreases monotonically with decreasing velocity. This sequence is repeated from 76 m/sec to 28 m/sec. A third tone begins at 42 m/sec and is still developing at 28 m/sec. Each tone peaks at about 1500 Hz.

The first tone that develops corresponds to the first lengthwise vortical-acoustic mode (n = 1) and has a bandwidth of about 50 Hz which increases slightly as velocity decreases. The second tone begins at 76 m/sec and has a bandwidth of about 300 Hz. Thus, as the velocity decreases, the cavity continues in oscillation by going to a higher mode. The bandwidth of the noise increases with decreasing velocity as in the case of vortex shedding from a cylinder. The frequency at which the maximum amplitude occurs

does not change with velocity but appears to be a characteristic parameter of the cavity (see eq. (5)).

The level of the tone as a function of velocity is shown in figure 6 for the first and second modes. Circles represent the first mode (n = 1) and triangles represent the second mode (n = 2). The velocity at which the amplitude is maximum for both modes corresponds approximately to the Mach number (eq. (7)) where the curves for lengthwise and depthwise oscillations intersect. (See fig. 4(a) where L/D = 0.66.) This indicates that coupling between the two types of oscillation does exist and results in amplification of the tone considerably greater for the first mode than for the second. The onset Mach number occurs at a lower value. The velocity range over which the oscillation occurs depends on the Q-factor of the cavity, which is discussed in the next section, and, as seen here, on the mode in which the cavity is oscillating.

Effect of Cavity Dimensions on Radiated Noise

Rectangular cavities.- Insight regarding the effect of cavity dimensions on the shape of the noise spectrum can now be gained by fixing two of the cavity dimensions and varying the other one. The parameters commonly used to characterize the cavity are length-to-depth ratio L/D and length-to-width ratio L/W.

The effect of changing the width of the cavity on the radiated noise spectrum may be seen in figure 7. Figure 7(a) shows the noise spectra of two cavities whose L/D ratio is 1.08. In figure 7(b) the L/D ratio is 2.00. Both figures 7(a) and 7(b) show a composite plot of the noise spectra of two cavities of different widths as well as the background noise spectrum. In figure 7(a) the wider cavity (L/W = 0.541), whose noise spectrum is shown by the dashed line, appears to be transparent to the flow feedback mechanism at the highest velocity. When the width is decreased (L/W = 1.00) at the same velocity, intense tones are generated.

At each of the four test velocities, the narrower cavity (higher L/W) continues to generate the more sharply defined tonal spectra. Similar results are seen in figure 7(b) where the sequence is repeated on a longer cavity. Again the narrower cavity (L/W = 1.85), indicated by the solid line, generates noise of a more tonal composition than the wider cavity (L/W = 1.00).

Within each frame in figures 7(a) and 7(b), the wide and narrow cavities peak at the same frequency; thus, the resonance frequency is not related to the width. Since the depth remains fixed for all spectra shown in figure 7 and since the location of the peaks does change from figures 7(a) to 7(b), it is evident that the frequency of this resonance is most dependent on the length.

However, the ratio of the center frequency to the bandwidth of the peak (called the Q or quality factor in reference to oscillators) does appear to be related (inversely) to the

13

cavity width. This relationship is characteristic of both standing-wave oscillators and Helmholtz oscillators and gives evidence that this type phenomenon is present. Therefore the narrow cavities have a higher Q. They begin oscillation at a higher velocity (first frame of fig. 7(a)) and still maintain a tonal spectra at the lower velocities (last frame of fig. 7(b)). Consequently, narrower cavities oscillate over a larger Mach number range. Also the cavity width appears to determine whether the cavity acts as a narrowband or broadband source at a given velocity.

Radiation from circular cavity.- In the two-dimensional model from which the vortical-acoustic modes were derived (in appendix B), it is understood that the leading and trailing edges of the cavity are parallel to each other but perpendicular to the flow. In this study, the effect of nonparallel edges was investigated by using a square and circular cavity of 7.62-cm length and diameter, respectively. The noise spectra from each of these cavities are plotted with the background noise spectra at three velocities in figure 8. The square and circular cavities have the same ratios of L/D, L/W, and W/D since the diameter of the circular cavity was used for the length and width of the square cavity. The spectra peak at the same frequency. The square cavity generates the more tonal spectrum. However, the circular-faced cavity generates slightly more overall noise. Thus, it not only appears that the parallel leading and trailing edges of the cavity are required for a strong feedback cycle but also that alteration of one or both edges considerably alters the type of mechanism generating most of the noise.

CONCLUDING REMARKS

The data of this experiment show an increasing Strouhal number with increasing cavity length-to-depth ratio (contrary to a previous investigation). This experimental trend prompted an extension of a previous analytical study to include the effect of length-to-depth ratio (L/D) in the prediction of the Strouhal number for lengthwise vortical-acoustic oscillation. The resulting expression yielded the same trend found in the data and agreed reasonably well with the data.

The expression for frequencies of the depthwise standing-wave modes was written in Strouhal form based on cavity length and plotted as a function of Mach number along with the Strouhal number expression for the vortical-acoustic oscillation. The Mach number at which these curves intersect was obtained and was shown to be the velocity at which the maximum amplitude of the cavity response occurs. The onset Mach number has a slightly smaller value.

The Strouhal numbers of the data taken from the deeper cavities (L/D $\leq$ 1) tend to follow the prediction for the depthwise standing-wave oscillation, whereas the data from the longer cavities (L/D $\geq$ 1) agree better with the Strouhal prediction for the vortical-

acoustic oscillation. In the Mach number range from 0.1 to 0.5, interaction between the two types of oscillation is observed.

Development of the noise spectrum with velocity gives further evidence of the interaction between the vortical-acoustic and the depthwise standing-wave modes. The Mach number at which maximum sound radiation occurs corresponds closely to the intersection of the curves representing the two types of oscillation. Considerably more sound is produced at this Mach number than at a higher or lower velocity.

The shape of the noise spectrum depends on the shape of the cavity opening. The frequency of the peak of the noise spectrum depends on the streamwise dimension of the cavity. The quality factor or peakedness of the spectrum is dependent on the width, the narrower cavities producing the more tonal noise spectra. Narrower cavities oscillate over a larger Mach number range. Comparison of the noise spectra from a square and a circular-faced cavity showed that the square cavity generated the more tonal noise spectra, but the circular-faced cavity produces more overall noise, spreading the energy over a larger frequency range.

Langley Research Center
National Aeronautics and Space Administration
Hampton, VA 23665
October 8, 1976

APPENDIX A

CORRECTION TO L_w FOR FREQUENCIES OTHER THAN 1 kHz

This appendix is provided for those interested in obtaining the correct spectral shape and level across the entire frequency range. The conversion of measured pressure levels L_p to acoustic power levels L_w is made in the following way (see ref. 7):

$$L_w = L_p - 10 \log_{10} \frac{T}{T_o} + 10 \log_{10} \frac{V}{V_o}$$

$$+ 10 \log_{10}\left(1 + \frac{S\lambda}{8V}\right) + 10 \log_{10} \frac{B}{1000} - 14 \qquad (A1)$$

where

L_w sound power level of source under test, dB (re 1 pW)

L_p mean band pressure level, dB (re 20 μPa)

T reverberation time of room, sec

T_o = 1 sec

V volume of room, m^3

V_o = 1 m^3

λ wavelength at center frequency of one-third octave band, m

S total surface area of room, m^2

B barometric pressure, mbar

The correction applied to the data reported herein used the 1-kHz values for the reverberation time T and the wavelength λ. The additional correction to be applied for the other frequencies is given in figure A1.

APPENDIX A
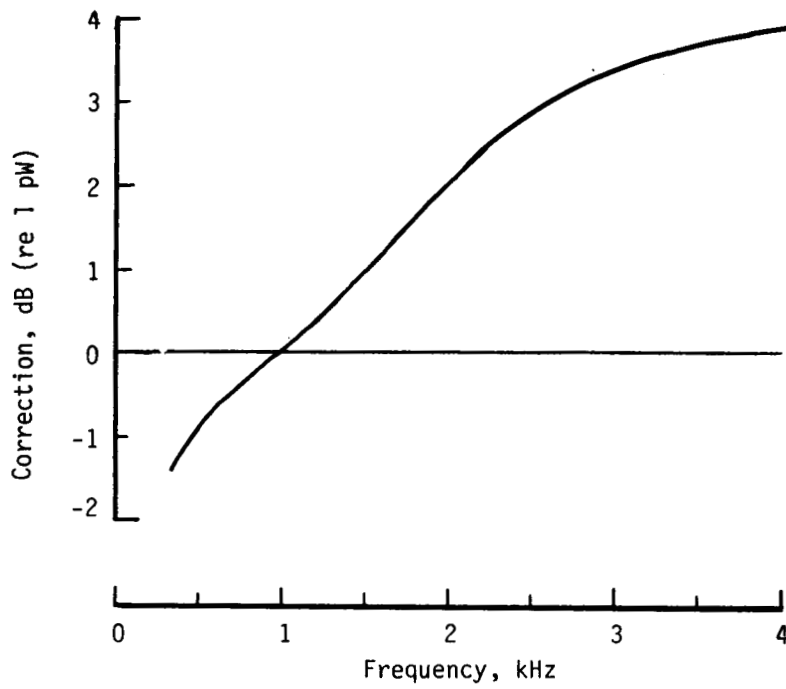
Figure A1.- Additional spectral correction to data obtained
in Langley 55-foot vacuum cylinder.

APPENDIX B

DERIVATION OF STROUHAL NUMBER FOR

VORTICAL-ACOUSTIC OSCILLATION

Consider a cavity as shown in the following sketch. The displacement of the thin shear layer which spans the cavity opening is assumed to take the form

$$\eta(x) \approx \exp k_i x \, \exp i\left(k_r x - \omega t + \phi\right) \tag{B1}$$

where k_r and k_i are the real and imaginary parts of the complex wave number in the x-direction and ϕ is the lag of the shear layer displacement behind the forcing mechanism at $x = 0$. The acoustic field is constructed by the method of images, the primary
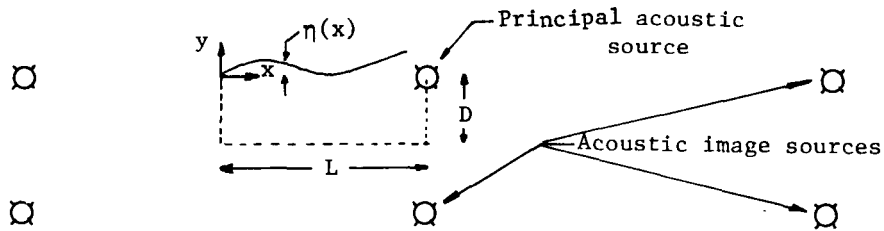
source being located at $x = L$, $y = 0$. This position is chosen because schlieren photographs (ref. 10) have shown sound waves emanating from the vicinity of this point. The boundary condition (normal velocity of 0 on the cavity walls) is met by placing additional sources at $y = 0$, $x = -L, \pm 3L, \pm 5L, \ldots$, at $y = -2D$, $x = \pm L, \pm 3L, \pm 5L, \ldots$, and so forth. The acoustic field produced by the sum of these two-dimensional sources is

$$P(x,y,t) = i\omega\rho S \exp(-i\omega t) \sum_{j=-\infty}^{\infty} \sum_{k=0}^{1} H_0^{(1)}\left\{\frac{\omega}{a}\left[\left(x - (2j+1)L\right)^2 + (y + 2kD)^2\right]^{1/2}\right\} \tag{B2}$$

where P is the acoustic pressure, a is the velocity of sound, and S is a constant related to the magnitude of the sources (ref. 3).

Trailing-Edge Condition

The source strength S is obtained by assuming that the strength of the monopole at the trailing edge ($x = L$, $y = 0$) is proportional to mass flux from shear layer displacement at the trailing edge. The mass flow rate per unit length for a single source is given by

$$\frac{\partial m}{\partial t} = \lim_{r \to 0} 2\pi r \rho U_r = \lim_{r \to 0} \frac{2\pi r}{i\omega} \frac{\partial P}{\partial r} = -4i\rho S \exp(-i\omega t)$$

where U_r is the radial component of velocity of the source and $\partial m/\partial t$ is the mass flux.

At the trailing edge the mass flux is assumed to be related to the shear layer displacement; that is,

$$\frac{\partial m}{\partial t} = C \, \eta(L,t) \exp(i\beta) = C \exp\left(k_i L\right) \exp i\left(k_r L - \omega t + \phi + \beta\right)$$

where the magnitude C would be dependent on fluid density, boundary-layer thickness, flow velocity, and cavity width, and where β is the difference in phase between the source and the shear layer displacement. Equating these expressions for $\partial m/\partial t$ yields for the source strength S

$$S = \frac{iC}{4\rho} \exp k_i L \exp i\left(k_r L + \phi + \beta\right) \tag{B3}$$

Then, the acoustic pressure (eq. (B2)) may be written

$$P(x,y,t) = \frac{\omega}{4} C \exp k_i L \exp i\left(k_r L + \pi + \phi + \beta\right) \exp(-i\omega t) \sum_{j=-\infty}^{\infty} \sum_{k=0}^{1} H_0^{(1)}\left\{\frac{\omega}{a}\left[\left(x - (2j+1)L\right)^2 + (y + 2kD)^2\right]^{1/2}\right\} \tag{B4}$$

Leading-Edge Condition

At the leading edge $(x = y = 0)$,

$$P(0,0,t) \propto \exp i\left(k_r L + \pi + \phi + \beta\right) \exp(-i\omega t) \sum_{j=-\infty}^{\infty} \sum_{k=0}^{1} H_0^{(1)}\left\{\frac{\omega}{a}\left[(2j+1)^2 L^2 + (2kD)^2\right]^{1/2}\right\} \tag{B5}$$

or

$$P(0,0,t) \propto \exp i\left(k_r L + \pi + \phi + \beta\right) \exp(-i\omega t) H \exp(ih) \tag{B6}$$

where H is the magnitude and h is the phase of the double sum on the right side of equation (B5). For the phase in equation (B6) to be consistent around the feedback circuit, the following relation must hold:

$$k_r L + \pi + \phi + \beta + h = 2n\pi \tag{B7}$$

Thus, to obtain a Strouhal relationship from this equation, an expression for h must be found.

In reference 3, h is obtained by considering the single source at the trailing edge of the cavity, that is, the first term of the sum of equation (B5). To include the effect of the depth, the following analysis also includes the source at $x = L$, $y = -2D$. Thus, the effect at the leading edge of the acoustic wave reflected from the bottom is taken into account. The phase h of the sum of the Hankel functions with argument corresponding to $j = 0$, $k = 0, 1$ can be written

$$h = \tan^{-1}\left\{\frac{Y_0\left(\frac{\omega L}{a}\right) + Y_0\left[\frac{\omega L}{a}\sqrt{1 + 2\left(\frac{D}{L}\right)^2}\right]}{J_0\left(\frac{\omega L}{a}\right) + J_0\left[\frac{\omega L}{a}\sqrt{1 + 2\left(\frac{D}{L}\right)^2}\right]}\right\} \tag{B8}$$

where J_0 and Y_0 are the Bessel functions of the first and second kind, respectively (order zero). The phase h is plotted in figure B1 as a function of $\omega L/a$ for several L/D ratios ranging from 0.25 to 8.0.

Obtaining Expressions for h and $N_{St,\ell}$

The phase h may be represented by a series about zero in $\omega L/a$ for a fixed value of L/D; that is,

$$h = h_0 + \frac{\omega L}{a}\,h_1 + \left(\frac{\omega L}{a}\right)^2 h_2 + \ldots \tag{B9}$$

Considering only the first two terms, it can be seen from figure B1 that h_0 is a constant but h_1, which represents the slope of h, changes with L/D. For small values of $\omega L/a$, it is seen that the slope decreases monotonically as the L/D ratio increases. The value of $\omega L/a$ for which a straight line is no longer a suitable representation of h is dependent on L/D. For example, for $L/D = 1$ the approximation is valid for $\omega L/a \le 2.0$.

To determine the applicability of such a representation, one must estimate the value of $\omega L/a$ for the experimental data. Typical values for $\omega L/a$ may be obtained from

$$\frac{\omega L}{a} = \frac{2\pi f L}{a} = \frac{2\pi L}{a}\left(\frac{N_{St,\ell}\, U_\infty}{L}\right) = 2\pi M N_{St,\ell} \qquad\qquad\text{(B10)}$$

where

$$N_{St,\ell} = \frac{fL}{U_\infty} \quad\text{or}\quad f = \frac{N_{St,\ell}\, U_\infty}{L}$$

Values of $\omega L/a$ for the Mach number range of the current test are tabulated as follows:

Mode number	Approximate $N_{St,\ell}$ (from fig. 3)	$\omega L/a$ (from eq. (B10))	$\omega L/a$ for $M \approx 0.4$
1	0.4	2.5M	1.0
2	.9	5.6M	2.2
3	1.5	9.4M	3.8
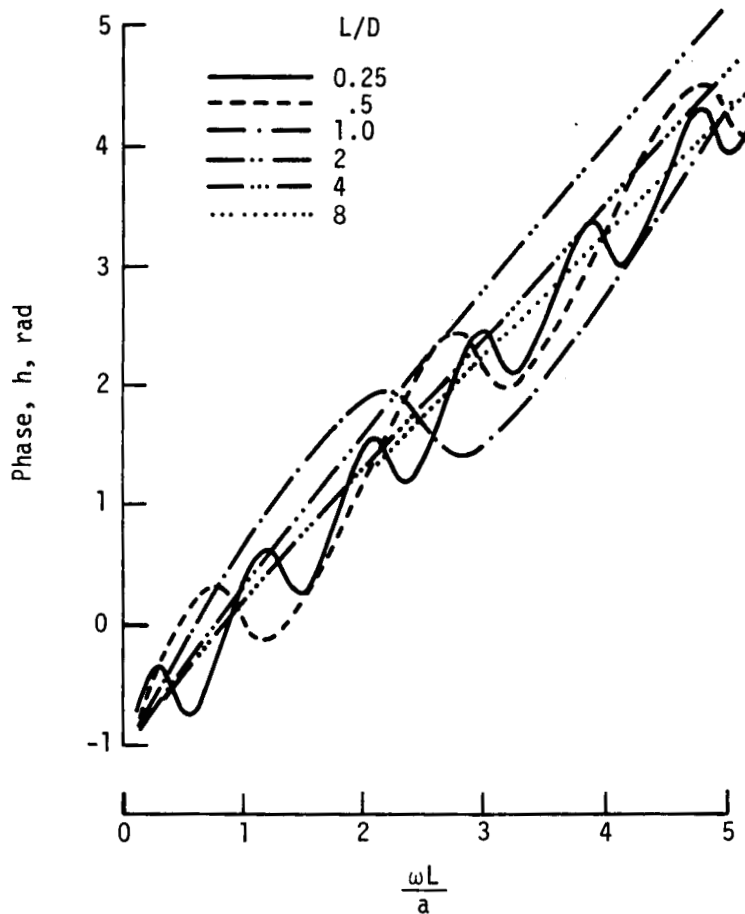
Figure B1.- Phase h as a function of $\omega L/a$ for several L/D ratios.

The right column gives typical conservative values of $\omega L/a$ associated with this test for each mode. Thus, for the first mode or stage of the vortical-acoustic oscillation, $\omega L/a = 1$ means that a straight-line approximation to the phase h is valid for cavities where the L/D is above about 1.0 (from fig. B1). As the mode number increases, the straight-line approximation is valid only at higher values of L/D. However, as seen in the text, cavities of small L/D resonate at much lower Mach numbers in the higher vortical-acoustic modes and thus inherently follow these restrictions.

By using the small argument approximation in equation (B8) to obtain h_0 and by estimating the slope h from figure B1, equation (B9) becomes

$$h\left(\omega L/a, \, L/D\right) = \frac{-\pi}{2} + \frac{\omega L}{a}\left(1 + \frac{0.514}{L/D}\right) \tag{B11}$$

Equation (B7) may then be solved for the Strouhal number to obtain

$$N_{St,l} = \frac{fL}{U_\infty} = \frac{n - \frac{1}{4} - \frac{\phi}{2\pi} - \frac{\beta}{2\pi}}{\frac{1}{k_r} + M\left(1 + \frac{0.514}{L/D}\right)}$$

The phase difference between the acoustic source and the positive shear layer displacement of the trailing edge (β) is taken to be $-\pi/2$. This value was chosen since it is reasonable to assume that the vortex is shed when the shear layer is one-quarter cycle from the zero position; however, this relationship may change with cavity length and the mode of oscillation. The phase difference ϕ between the acoustic wave arrival and vortex sheet displacement at $x = 0$ is assumed to be small enough to be neglected. The Strouhal relationship becomes

$$N_{St,l} = \frac{n}{\frac{1}{k_r} + M\left(1 + \frac{0.514}{L/D}\right)} \tag{B12}$$

Equation (B12) is an expression for the Strouhal number which includes the effect of the bottom-reflected acoustic wave that originated at the trailing edge. The analysis gives results for the case where both waves arrive at the leading edge equally weighted.

Equation (B12) may be improved in two areas. First, the phase relationship between the shear layer displacement and the sound generation needs to be determined as a function of mode number n. Evidence for this type of dependence comes from detailed studies of the edgetone phenomenon. Second, the vortex convection velocity, chosen herein to be a constant, is more likely a function of cavity length and flow velocity.

REFERENCES

1. Block, Patricia J. W.; and Heller, Hanno: Measurements of Farfield Sound Generation From a Flow-Excited Cavity. NASA TM X-3292, 1975.

2. Rossiter, J. E.: Wind-Tunnel Experiment on the Flow Over Rectangular Cavities at Subsonic and Transonic Speeds. R. & M. No. 3438, British A.R.C., Oct. 1964.

3. Bilanin, Alan J.; and Covert, Eugene E.: Estimation of Possible Excitation Frequencies for Shallow Rectangular Cavities. AIAA J., vol. 11, no. 3, Mar. 1973, pp. 347-351.

4. Plumblee, H. E.; Gibson, J. S.; and Lassiter, L. W.: A Theoretical and Experimental Investigation of the Acoustic Response of Cavities in an Aerodynamic Flow. WADD-TR-61-75, U.S. Air Force, Mar. 1962.

5. East, L. F.: Aerodynamically Induced Resonance in Rectangular Cavities. J. Sound & Vib., vol. 3, no. 3, May 1966, pp. 277-287.

6. Schloth, Arthur P.: Measurements of Mean Flow and Acoustic Power for a Subsonic Jet Impinging Normal to a Large Rigid Surface. NASA TM X-72803, 1976.

7. American National Standard Methods for the Determination of Sound Power Levels of Small Sources in Reverberation Rooms. S1.21-1972, American Natl. Stand. Inst., Inc., [1972].

8. Heller, H. H.; Holmes, D. G.; and Covert, E. E.: Flow-Induced Pressure Oscillations in Shallow Cavities. J. Sound & Vib., vol. 18, no. 4, Oct. 1971, pp. 545-553.

9. Heller, Hanno H.; and Bliss, Donald B.: The Physical Mechanism of Flow-Induced Pressure Fluctuations in Cavities and Concepts for Their Suppression. AIAA Paper 75-491, Mar. 1975.

10. Krishnamurty, K.: Acoustic Radiation From Two-Dimensional Rectangular Cutouts in Aerodynamic Surfaces. NACA TN 3487, 1955.

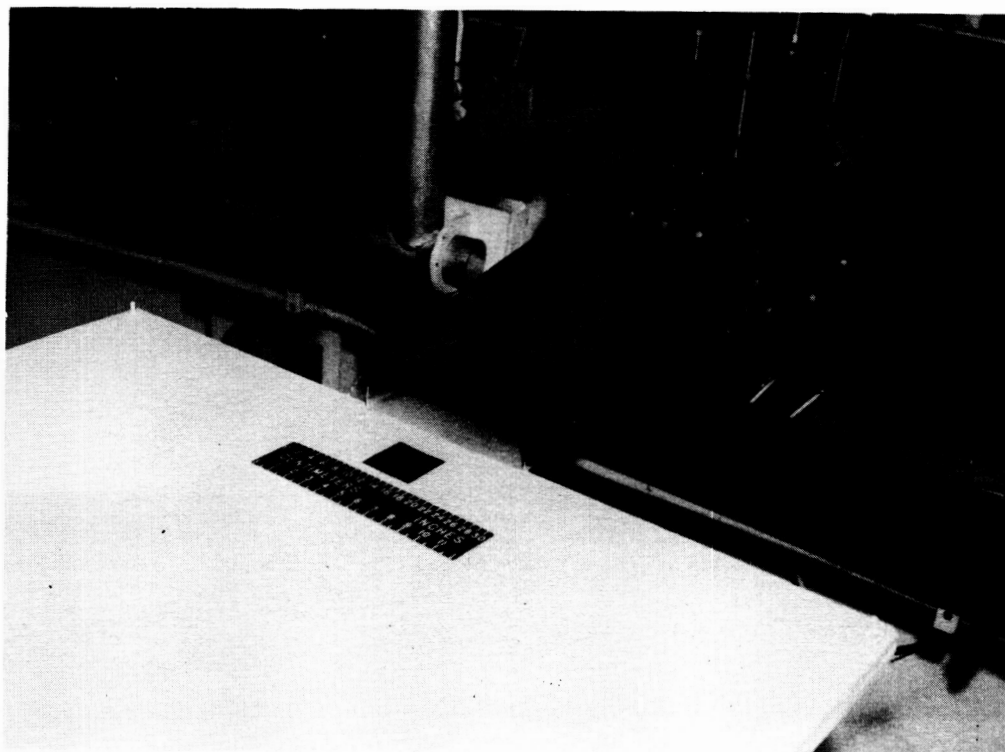## TABLE I.- TEST CONDITIONS IN LANGLEY 55-FOOT VACUUM CYLINDER

Dimensions, cm			L/D	Average flow velocity, m/sec
			Square cavity	
L	W	D		
4.13	4.13	3.81	1.08	168, 122, 84, 63, 42, 32, 21
7.62	4.13	3.81	2.00	163, 121, 84, 61, 40, 28, 16
4.13	7.62	3.81	1.08	169, 121, 83, 61, 30, 24
7.62	7.62	3.81	2.00	171, 123, 88, 64, 49, 38, 30
2.54	7.62	3.81	.66	178, 168, 147, 122, 113, 106, 91, 85, 82, 76, 69, 61, 51, 47, 42, 36, 30, 28, 21
			Circular cavity	
Diameter	D			
7.62	3.81		----	171, 122, 104, 85, 62, 44, 32, 23

TABLE II.- TEST CONDITIONS IN LANGLEY ANRL REVERBERATION ROOM

Cavity depth, D, cm	L/D	Flow velocity, m/sec
0.5	8.1	32, 40, 48, 57, 65
1.0	4.0	32, 40, 48, 57, 65
2.0	2.025	32, 40, 48, 57, 65
3.0	1.35	32, 40, 48, 57, 65
4.0	1.01	32, 40, 48, 57, 65
5.0	.81	32, 40, 48, 57, 65
6.0	.675	32, 40, 48, 57, 65
8.0	.5	32, 40, 48, 57, 65
10.0	.4	32, 40, 48, 57, 65
13.0	.312	32, 40, 48, 57, 65
Cavity length, L = 4.05 cm, Cavity width, W = 7.45 cm		
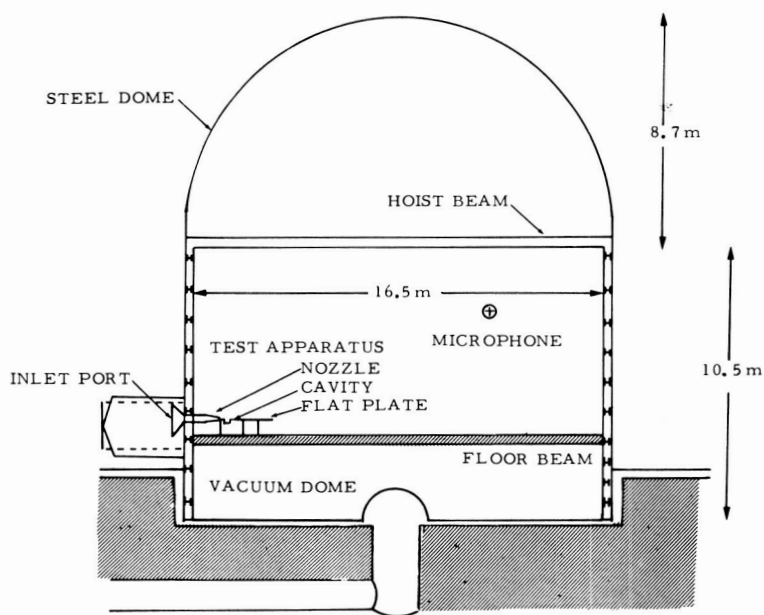
(a) Facility.

(b) Test setup.

L-74-8679

Figure 1.- Langley 55-foot vacuum cylinder and test setup.

L-75-2067

(b) Test setup.

(a) Facility.

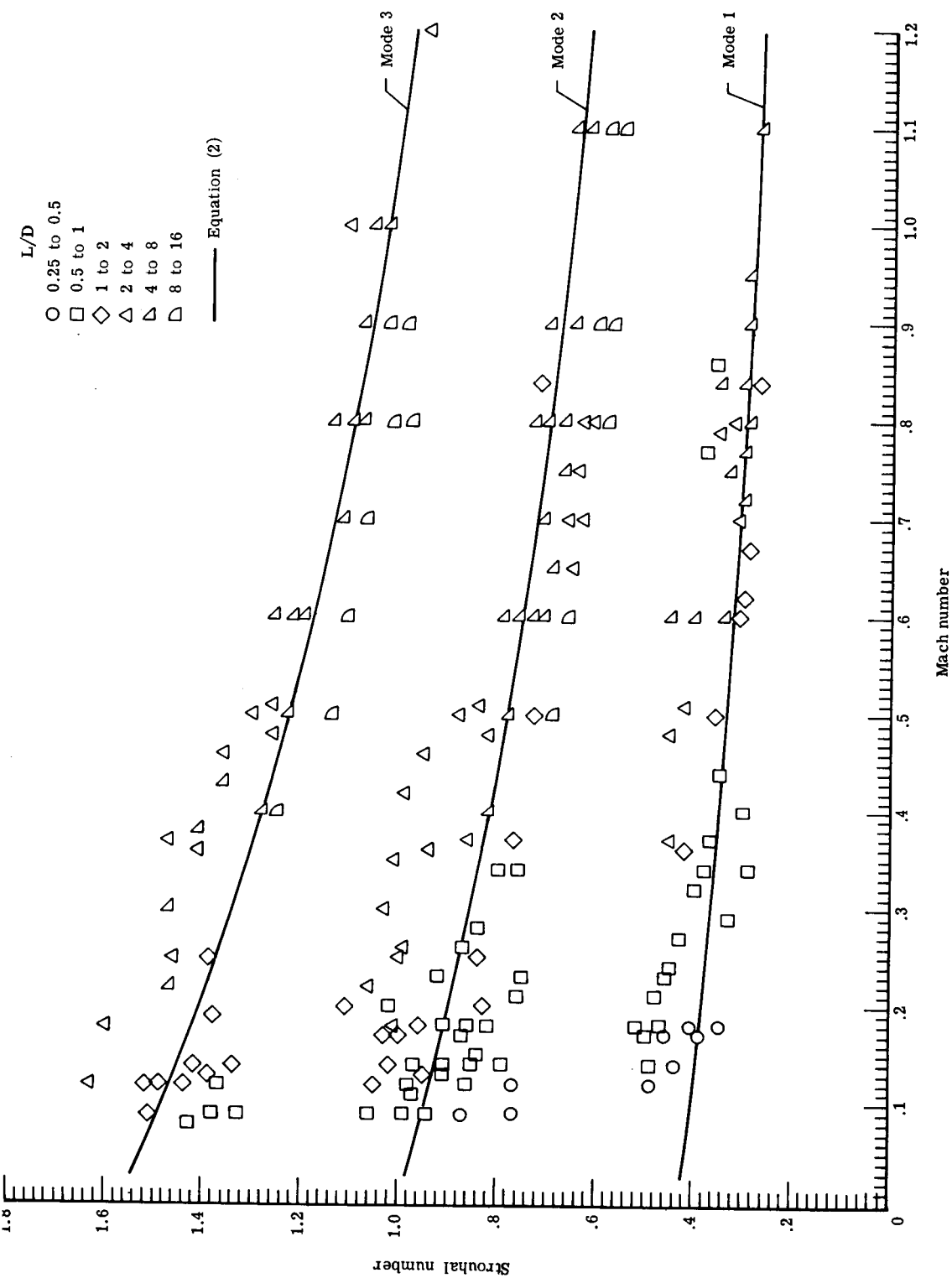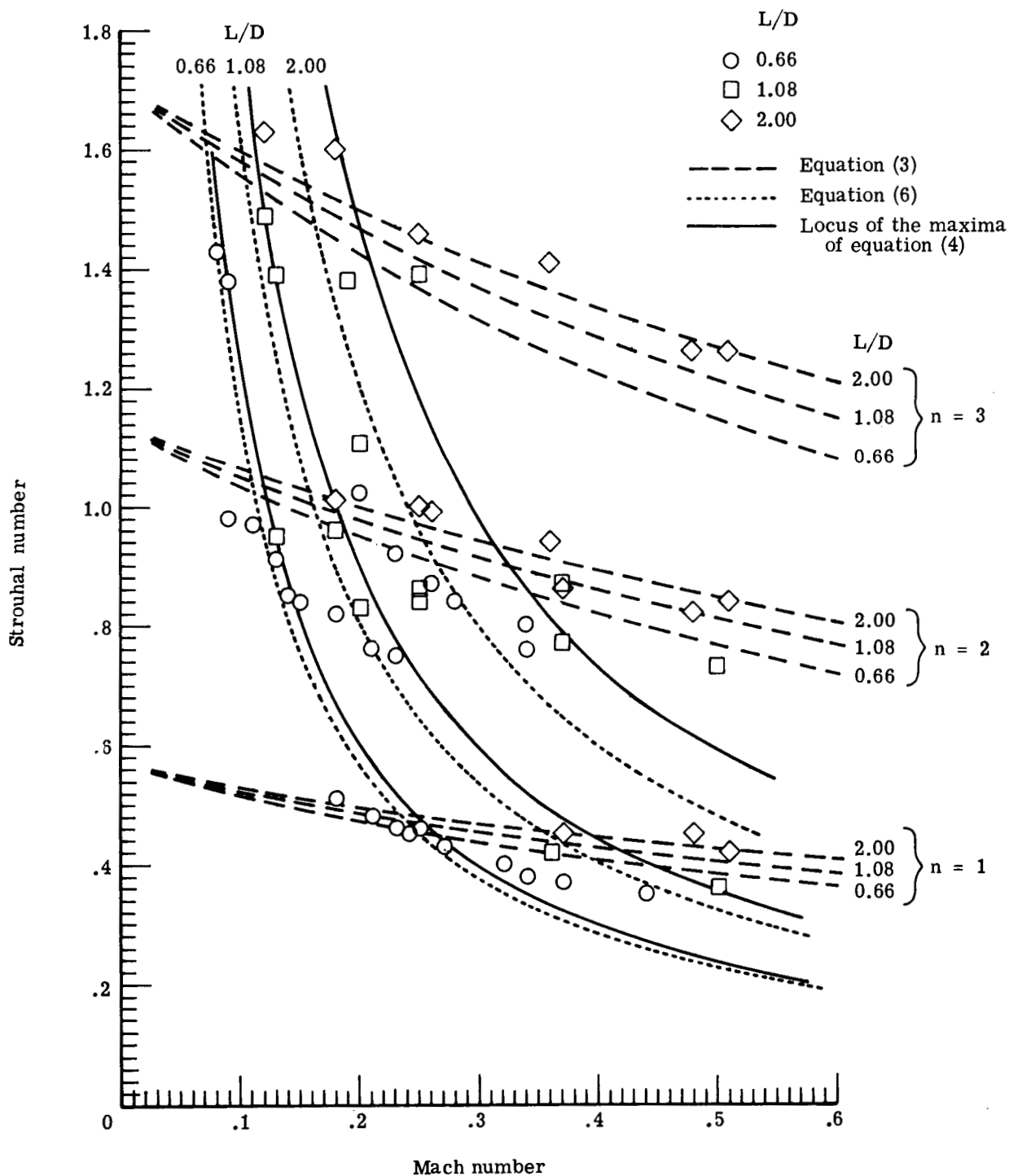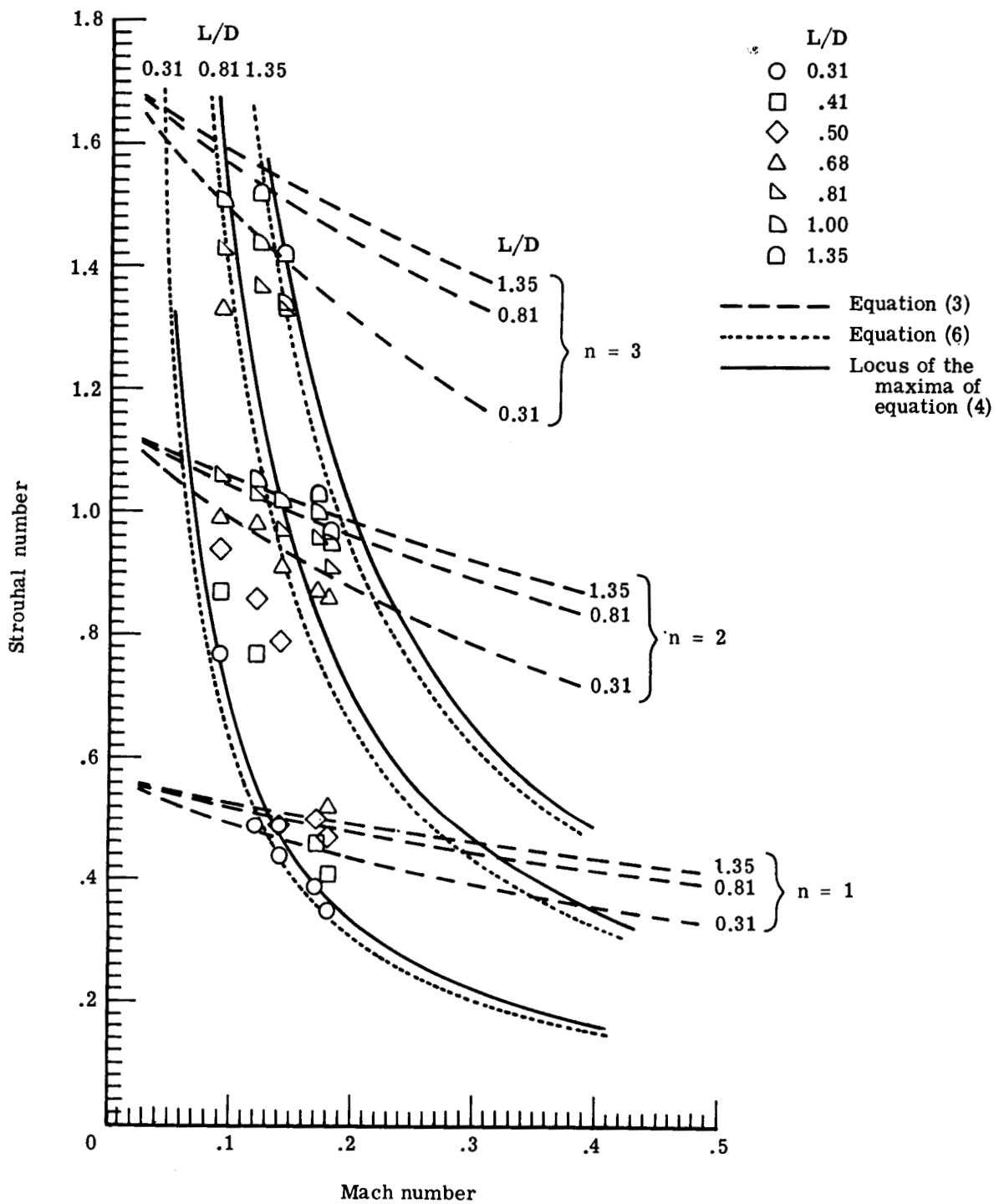Figure 2.- Langley ANRL reverberation room and test setup.

Figure 3.- Experimental results from several investigations of cavity oscillation frequencies compared with prediction of equation (2).

27

(a) Data from Langley 55-foot vacuum cylinder.

Figure 4.- Comparison of current data with equations (3) and (6).

(b) Data from Langley ANRL reverberation room.

Figure 4.- Concluded.
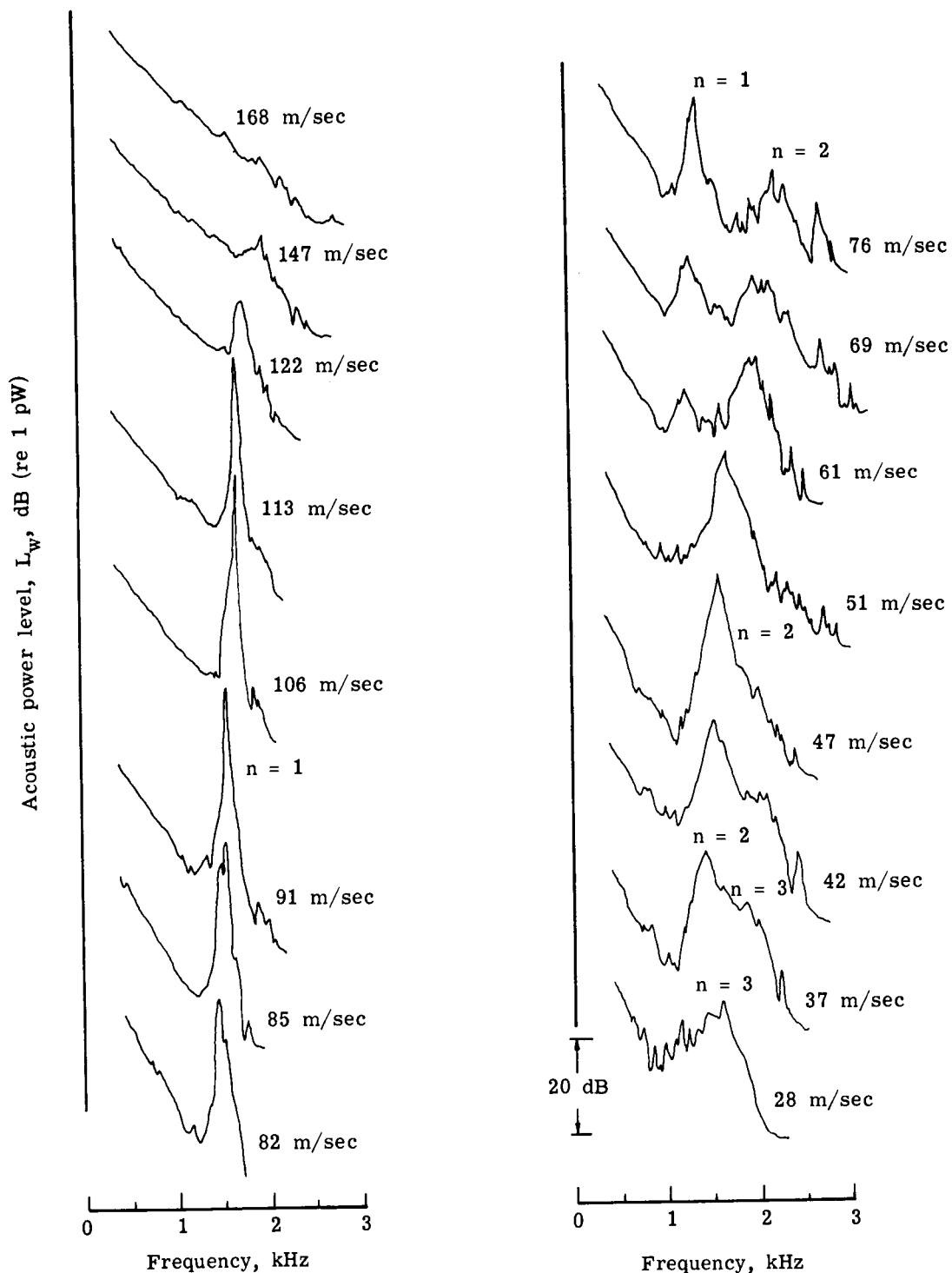
Figure 5.- Sequence of power spectra showing change in spectral modes and shape with velocity. L = 2.54 cm;   W = 7.62 cm;   D = 3.81 cm;   L/D = 0.66.
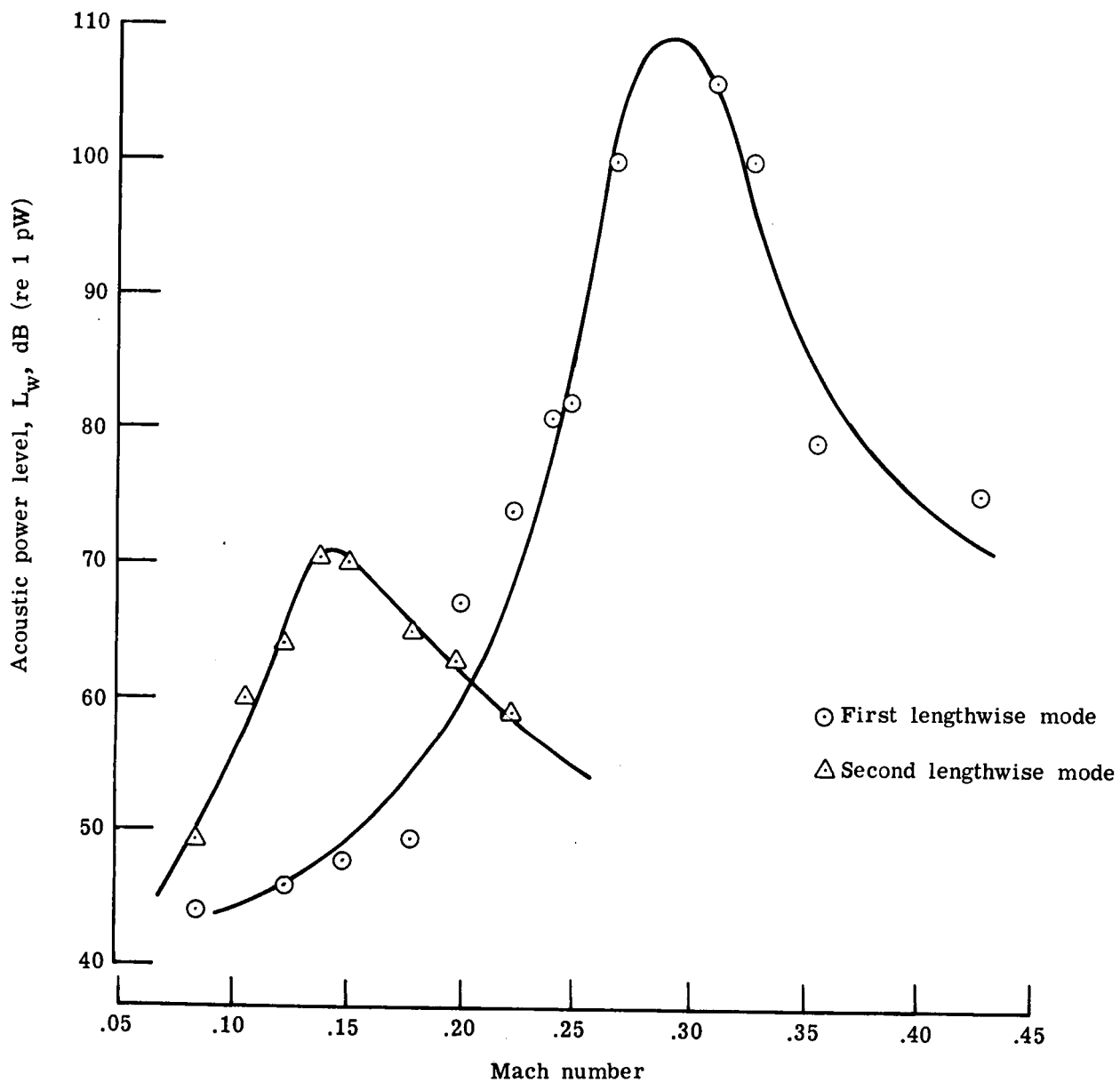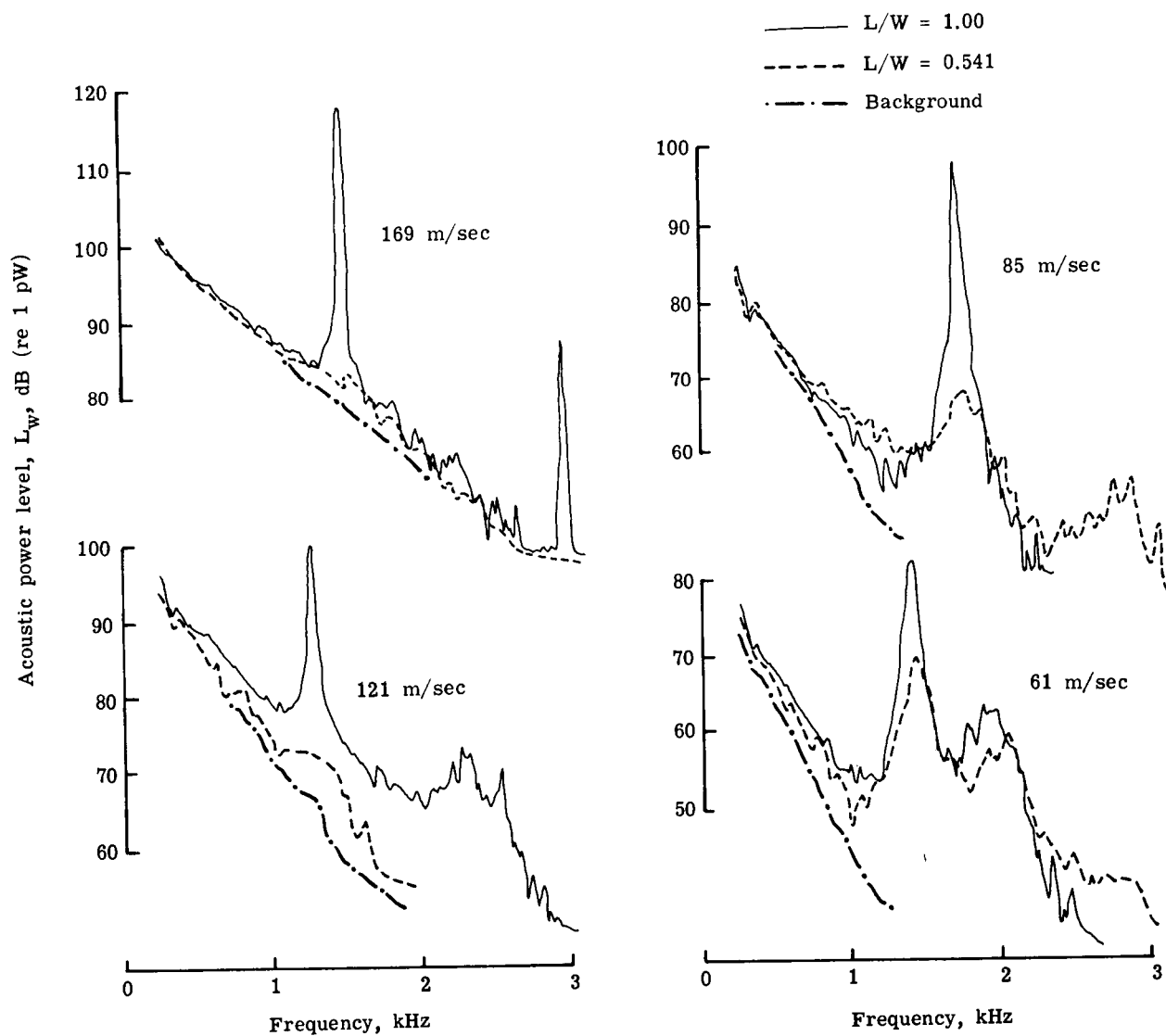
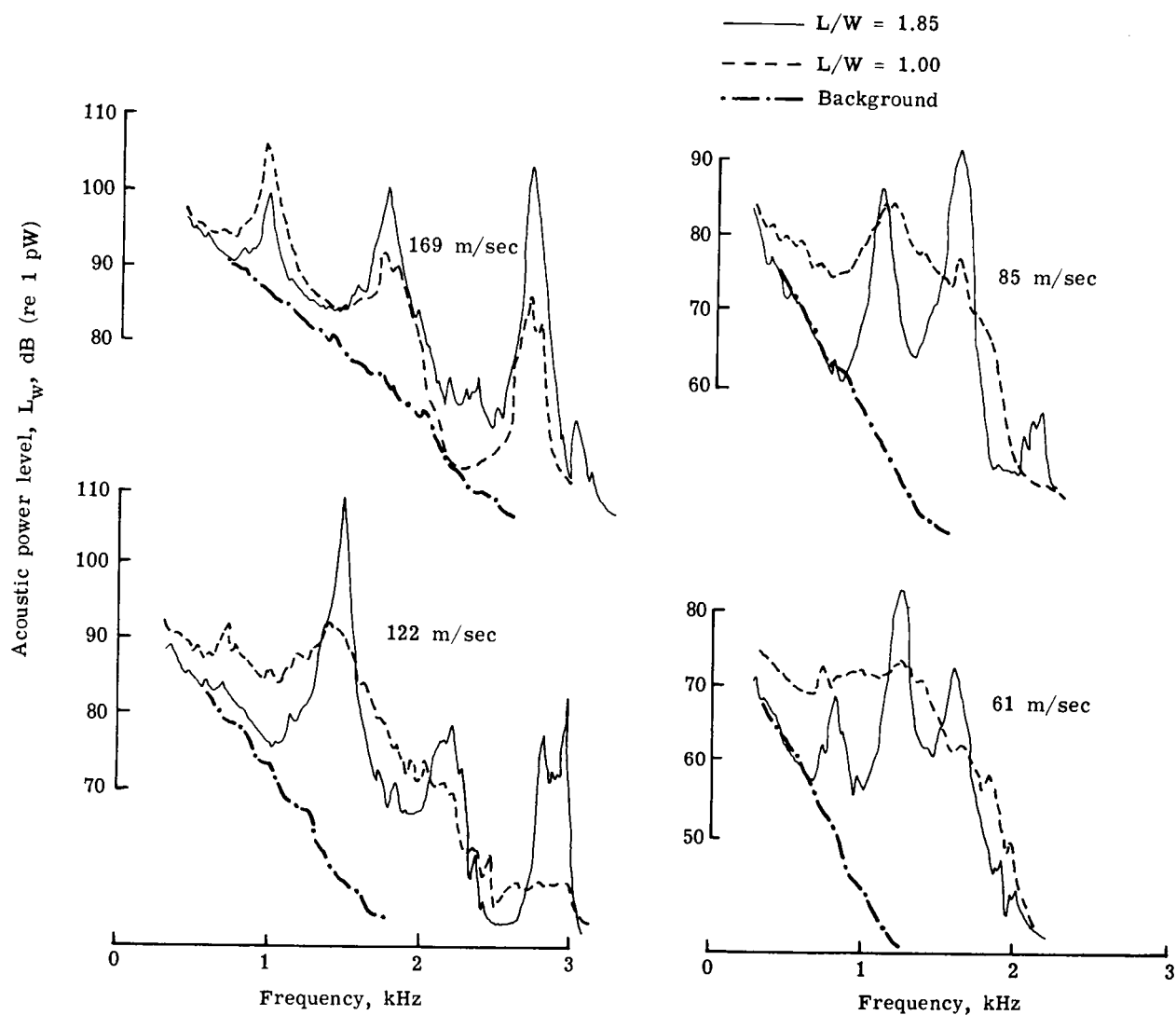Figure 6.- Change in the amplitude of tone generated by cavity as a function of velocity. L = 2.54 cm;   W = 7.62 cm;   D = 3.81 cm;   L/D = 0.66.

(a) L = 4.13 cm;   D = 3.81 cm;   L/D = 1.08.

Figure 7.- Effect of changing cavity width (cross-stream dimension)
on radiated noise spectra.

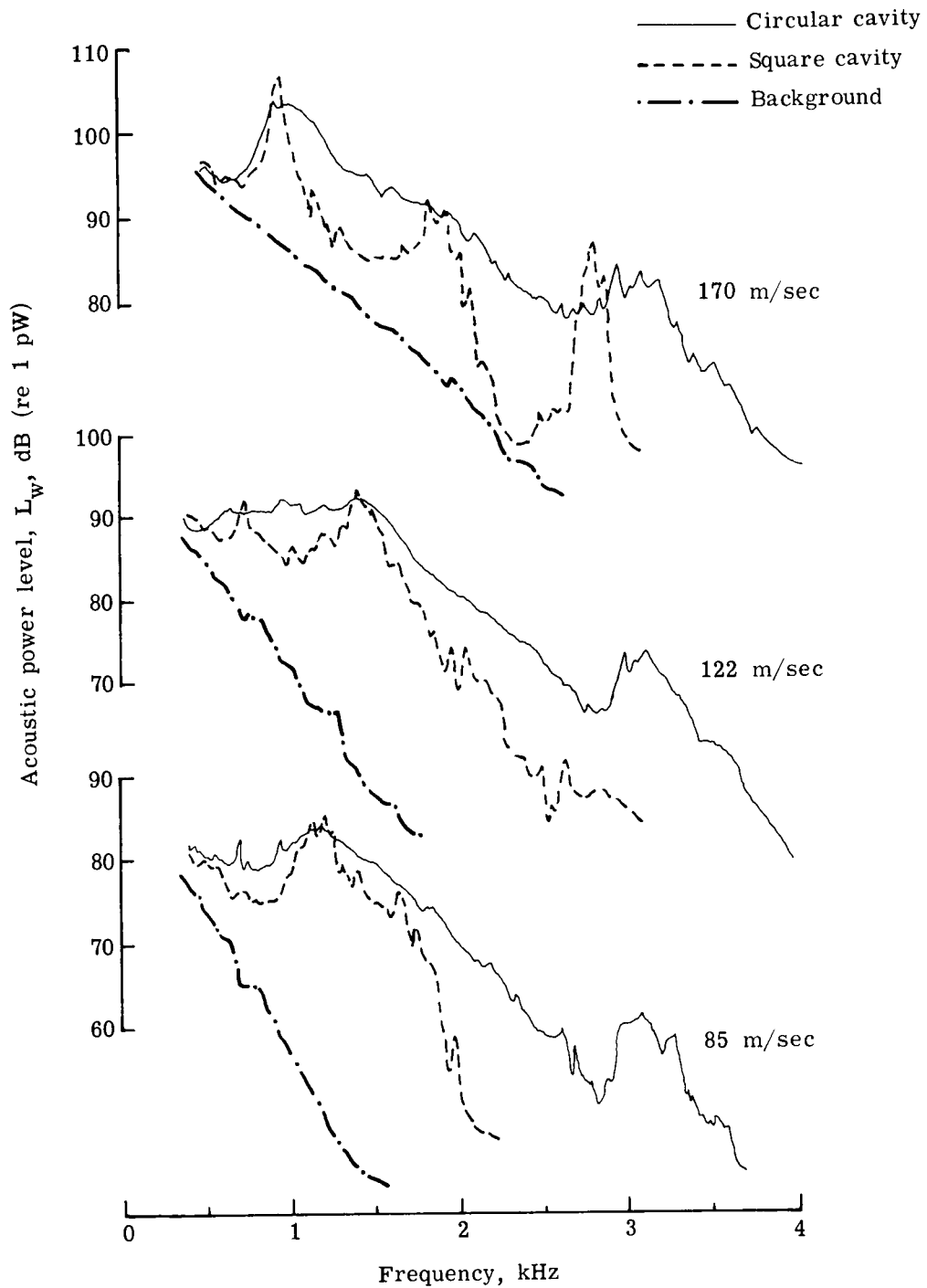(b)   L = 7.62 cm;   D = 3.81 cm;   L/D = 2.00.

Figure 7.- Concluded.

Figure 8.- Comparison of the noise from a square and a circular-faced cavity of equal depth and streamwise dimension.

1. Report No. NASA TN D-8351	2. Government Accession No.	3. Recipient's Catalog No.
4. Title and Subtitle NOISE RESPONSE OF CAVITIES OF VARYING DIMENSIONS AT SUBSONIC SPEEDS		5. Report Date December 1976
		6. Performing Organization Code
7. Author(s) Patricia J. W. Block		8. Performing Organization Report No. L-11045
9. Performing Organization Name and Address NASA Langley Research Center Hampton, VA 23665		10. Work Unit No. 505-03-12-03
		11. Contract or Grant No.
12. Sponsoring Agency Name and Address National Aeronautics and Space Administration Washington, DC 20546		13. Type of Report and Period Covered Technical Note
		14. Sponsoring Agency Code

15. Supplementary Notes

16. Abstract

An expression for the Strouhal number of lengthwise cavity oscillations is obtained which includes the effect of length-to-depth ratio. This expression, which agrees well with the experimental data, is also used to predict the Mach number at which cavity acoustic response is maximum. Interaction between lengthwise and depthwise modes is seen to occur at Mach numbers from 0.1 to 0.5. Cavity shape is shown to effect the noise spectra in generating either a broadband or narrowband signal.

7. Key Words (Suggested by Author(s)) Cavity noise Airframe noise Aerodynamic noise	18. Distribution Statement Unclassified — Unlimited
	Subject Category 71

3. Security Classif. (of this report) Unclassified	20. Security Classif. (of this page) Unclassified	21. No. of Pages 34	22. Price* $3.75